The effect of surface roughness on the adhesion of elastic plates with application to biological systems

B.N.J. Persson[1] and S. Gorb[2]
[1] *IFF, FZ-Jülich, 52425 Jülich, Germany*
[2] *MPI für Metallforschung, Heisenbergstr. 3, D-70569 Stuttgart, Germany*

We study the influence of surface roughness on the adhesion of elastic plates. Most real surfaces have roughness on many different length scales, and this fact is taken into account in our analysis. We consider in detail the case when the surface roughness can be described as a self affine fractal, and study the plate-substrate pull-off force as a function of the surface roughness. Based on the theoretical results we discuss adhesion in biological systems, focusing on the adhesive pads of lizards.

81.40.Pq, 62.20-x

1. Introduction

In this paper we discuss adhesion of an elastic plate to a hard randomly rough surface, which has many important applications, e.g., in biological systems [1]. We calculate the plate-substrate pull-off force under the assumption that there is complete contact in the nominal contact area. We assume that the substrate surface has roughness on many different length scales, and consider in detail the case of self affine fractal surfaces.

Adhesion of an elastic solid to a rough substrate involves the competition between the (negative) attractive adhesion energy, which result mainly from the regions where the two solids are in atomic contact at the interface, and the (positive) repulsive elastic energy associated with the bending of the surface of the elastic solid so that it comes in direct atomic contact with the substrate. Thus, if A_0 is the nominal contact area between the solids and A the true atomic contact area, then we define the effective interfacial energy

$$\gamma_{\rm eff} A_0 = \Delta\gamma A - U_{\rm el}$$

Here $\Delta\gamma = \gamma_1 + \gamma_2 - \gamma_{12}$ is the change in the interfacial energy (per unit area) when *perfectly flat* surfaces of the two solids are brought into contact, and $U_{\rm eff}$ is the elastic (bending) energy necessary in order to make atomic contact at the interface. In this paper we will assume complete contact between the solids in the nominal contact area so that $A = A_0$. The more general problem of partial contact was studied in Ref. [2] for semi infinite solids. We plan to extend the study in Ref. [2] to the thin-plate case considered in this paper.

The theory we develop in this paper can be applied to biological adhesion systems, e.g., to the adhesion pads of flies, beetles, spiders or lizards. In particular, we focus on the adhesion of the gecko foot pad to surfaces with random roughness. This seams to be a case of "dry" adhesion, where no fluid is injected in the contact area, and is hence a particularly simple and well-defined system [3]. The skin of on the gecko foot pad is made from keratin-like protein with an elastic modulus of order $E \approx 10^9$ Pa. This is much higher than the elastic modulus of rubber, where typically $E \approx 10^6$ Pa. However, even for rubber a relative small surface roughness (of order a few micrometer root-mean-square amplitude) is able to completely eliminate the adhesion, resulting in zero pull-off force [4]. How, then, is it possible for the lizard to adhere even to a very rough stone wall when the elastic modulus of the pad skin is much higher than that of rubber?

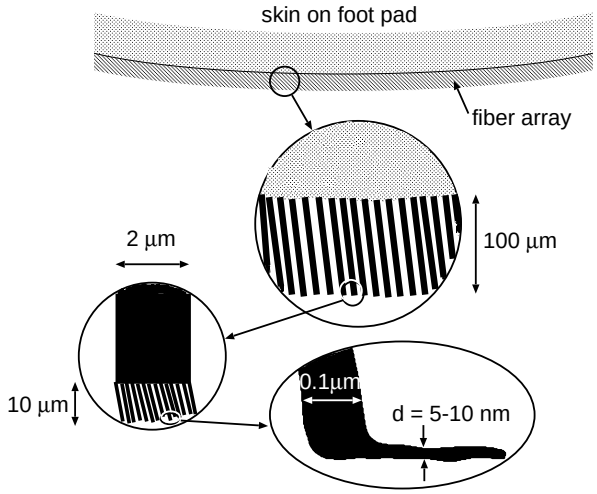

FIG. 1. Schematic picture of the lizard adhesive system. The skin of the lizard is covered by a dense layer of thin fibers or hair (setae) (length ≈ 100 μm and width of fiber of order ~ 1 μm). Each of these fibers branch out into about 1000 thinner fibers (length ~ 10 μm and width of order ~ 0.1 μm). Each of the thin fiber ends with a thin $(5-10$ nm) leaf-like plate (spatula).

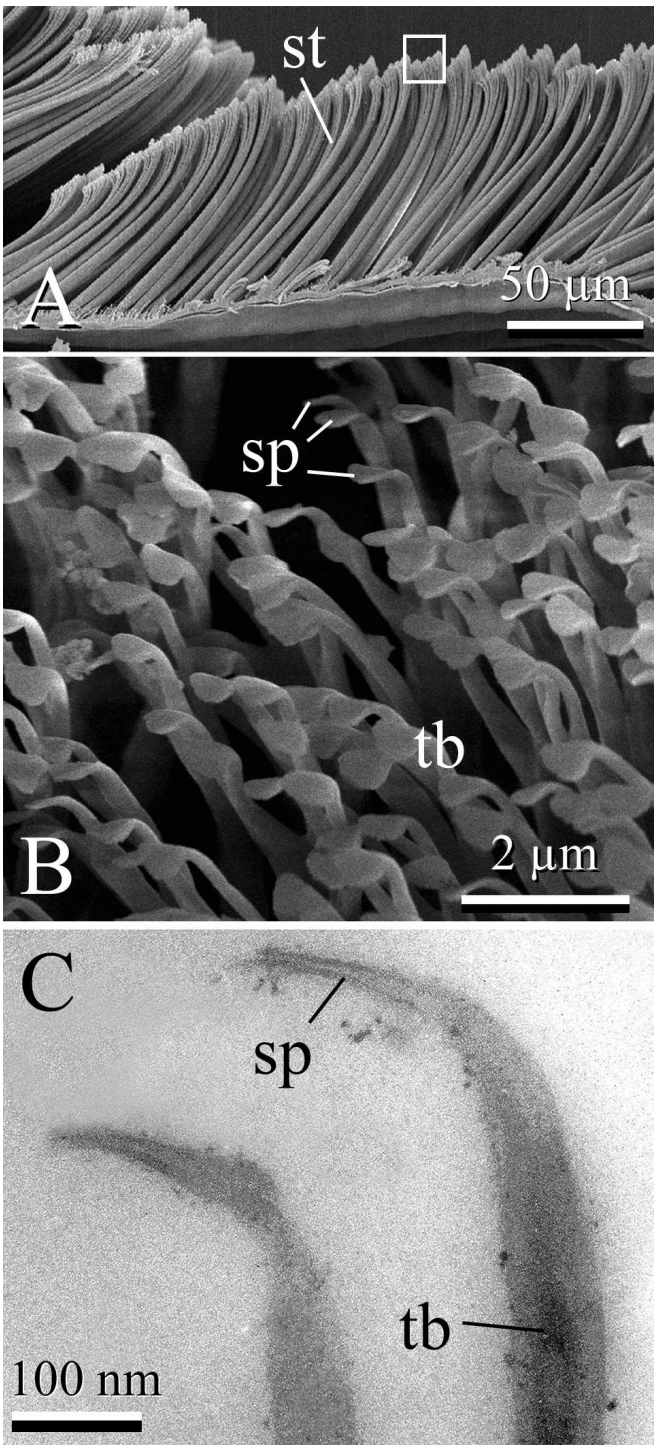

FIG. 2. Details of attachment system of the tokay gecko (Gekko gecko). A. Scanning electron microscopy (SEM) micrograph of setae (st) located on thin keratin film. B. Magnification (SEM micrograph) of the area surrounded by the white rectangle in A, showing terminal branches (tb) of setae with the spatulae (sp). C. Transmission electron microscopy micrograph of ultrathin section of two terminal branches (tb) with spatulae (sp).

During millions of years of evolution, driven by natural selection, an extremely soft elastic layer has appeared on the lizard pad surface. This layer is built in a hierarchic manner from fibers and plates, see Figs. 1 and 2. The hierarchic nature of the adhesive system reflect the hierarchic nature of most natural surfaces (to which the lizard must be able to adhere), which have roughness on all length scales, from the macroscopic scale (e.g., size of the lizard toe pad) down to the atomic scale. Thus, the skin of the lizard pad is covered by a dense layer of fibers or hair (satea) (length ≈ 100 μm and width ~ 1 μm). Each of these fibers branch out into about 1000 thinner fibers (length ~ 10 μm and width ~ 0.1 μm). Each of these thin terminal fibers ends with a thin $(5-10$ nm) leaf-like plate (spatula). This hierarchical construction makes the lizard adhesive system elastically very soft on all relevant length scales (from mm to nm).

In an earlier paper one of us has studied how the elastic bending energy stored in the setae fiber array systems influence the pull-off force [5]. The force necessary to remove an individual setae (or spatula) was assumed known (e.g., obtained from experiments). In this paper we focus instead on the binding between the spatula leaf-like plate and the substrate.

2. Pull-off force

Consider an elastic plate (thickness d) in contact with a rough but nominal flat substrate. The plate is able to bend to follow the substrate roughness wavelength components λ which are much larger than the thickness d of the plate. Let us first estimate the pull-off force F when the plate is in contact with a smooth (flat) substrate, and the with l of the detached region is large compared to the thickness d of the plate, see Fig. 3(a). The total energy

$$U = -\Delta\gamma B(L_0 - x) + Fx(1 - \cos\alpha),$$

where B is the width of the plate-like structure and L_0 the length, and $\Delta\gamma = \gamma_1 + \gamma_2 - \gamma_{12}$ the change in surface energy when the plate makes contact with the substrate. The pull-off force is determined by the condition $\partial U/\partial x = 0$ which gives

$$F = \frac{\Delta\gamma B}{1 - \cos\alpha}$$

The perpendicular force

$$F_\perp = F\sin\alpha = \frac{\Delta\gamma B\sin\alpha}{1 - \cos\alpha} \qquad (1)$$

Eqs. (1) and (2) are also valid for rough substrates if we replace the interfacial surface energy difference $\Delta\gamma$ with the effective surface energy $\gamma_{\rm eff}$ defined in Sec. 1. In Fig. 4 we show the (perpendicular) pull-off force as a function of the angle α. Note that $F_\perp \to \infty$ as $\alpha \to 0$. The reader can immediately verify this equation by pulling off a Scotch tape from a flat substrate at different pulling angles α. Eq. (1) also explain one reason for why the legs

of the lizard point outwards, away from the body; this makes α small and the vertical pull-off force large.

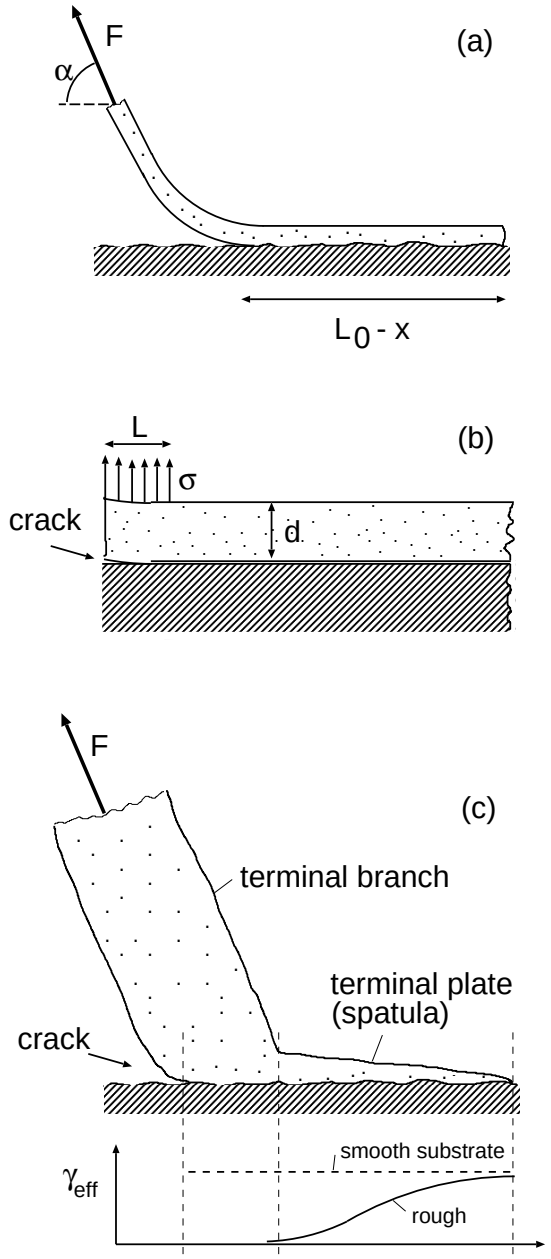

FIG. 3. (a) A thin plate pulled off a substrate (pull-off force F). (b) The initial force, when the length l of the crack is much shorter than the thickness d of the plate, is much higher than the force in (a) where $l >> d$. (c) A thin fiber in contact with a relatively smooth substrate. The fiber ends with a thin plate-like structure (spatula) (thickness of order 5-20 nm) which is able to deform to follow the substrate roughness profile. The effective interfacial surface energy, $\gamma_{\rm eff}$, depends on the thickness of the terminal plate, and we expect $\gamma_{\rm eff}$ to vary with the location along the spatulae as indicated by the solid line in the bottom part of the figure.

The initial force to "nucleate" the crack at the plate edge [see Fig. 3(b)] is higher than the "steady-state" pull-off force F shown in Fig. 3(a). Thus, if the crack length $l << d$ and if the perpendicular stress σ act over a region of length $L > d$ we have the standard result

$$\sigma \approx \left(\frac{E\Delta\gamma}{l}\right)^{1/2}$$

and the pull-off force

$$F = BL\sigma \approx BL\left(\frac{E\Delta\gamma}{l}\right)^{1/2} \qquad (2)$$

The spatula ends with an elastic leaf-like plate with the lateral dimensions of order 200-300 nm, and with a thickness which varies from $d \approx 20$ nm at the base to $d \approx 5$ nm at the tip, see Fig. 3(c). For a smooth substrate the spatulae is likely to adhere along its full length as indicated in the figure. In this case the force necessary in order to initiate pull-off is given by a formula similar to Eq. (2) with $B \approx L \approx D$ of order the thickness $D \approx 0.1$ μm of the terminal branch, and with an initial crack length equal to some small fraction of the diameter of the terminal branch, e.g., $l \approx 0.1D$. Using $\Delta\gamma \approx 2$ meV/Å^2 and $E \approx 10^9$ Pa, this gives the pull-off force of order 1 μN, which is close to the observed value for smooth substrates. On a rough substrate the interfacial free energy difference $\Delta\gamma$ must be replaced by the effective free energy $\gamma_{\rm eff}$ which includes the elastic energy stored at the interface. The latter depends on the thickness of the terminal plate, and we expect $\gamma_{\rm eff}$ to vary with the location along the spatulae as indicated in Fig. 3(c)(bottom, solid line). Thus, in this case effective adhesion may only occur to the tip of the terminal plate, and the pull-off force will be determined by this contact region by a formula of the type given by Eq. (1), but with $\Delta\gamma$ replaced by $\gamma_{\rm eff}$.

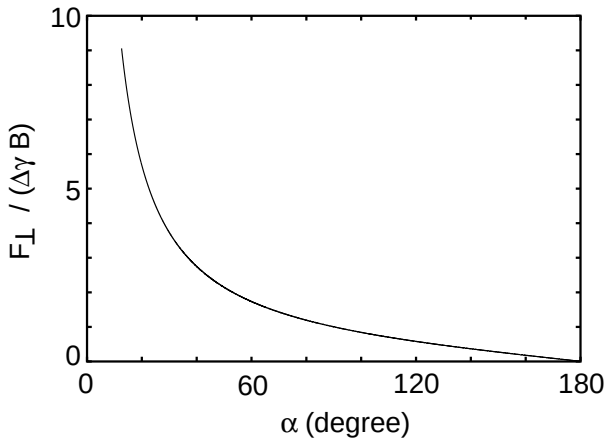

FIG. 4. The perpendicular pull-off force as a function of the angle α defined in Fig. 3.

3. Interfacial elastic and adhesion energies for rough surfaces

Assume that a thin elastic slab (thickness d) is in contact with the rough surface of a hard solid. Assume that because of the slab-substrate adhesion interaction, the slab deforms elastically and makes contact with the substrate everywhere, see Fig. 5.

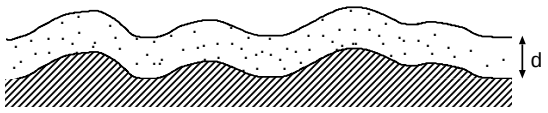

FIG. 5. The adhesion interaction pull the elastic slab into complete contact with the rough substrate surface.

Let us calculate the difference in the free energy between the slab in contact with the substrate and the non-contact case. Let $z = h(\mathbf{x})$ denote the height of the rough surface above a flat reference plane (chosen so that $\langle h \rangle = 0$). Assume first that the elastic slab is in direct contact with the substrate over the whole nominal contact area. Let us calculate the elastic energy stored in the deformation field in the elastic slab. We first assume that the thickness d of the slab is much smaller than the shortest wavelength λ associated with the substrate roughness profile. In this case we can use the theory of elastic plates to calculate the elastic energy. Let $z = u(\mathbf{x})$ denote the vertical displacement field of a thin plate, which originally (in the undeformed state) occupy the xy-plane. The elastic energy in the plate is given by [6]:

$$U_{\rm el} = \frac{Ed^3}{24(1-\nu^2)} \int d^2x \left[\left(\nabla^2 u\right)^2 - 2(1-\nu)|u_{ij}| \right] \quad (3)$$

where the determinant

$$|u_{ij}| = \frac{\partial^2 u}{\partial x^2}\frac{\partial^2 u}{\partial y^2} - \left(\frac{\partial^2 u}{\partial x \partial y}\right)^2$$

Let us write

$$u(\mathbf{x}) = \int d^2q \; u(\mathbf{q}) e^{i\mathbf{q}\cdot\mathbf{x}}$$

We get

$$\int d^2x \left(\nabla^2 u\right)^2 = (2\pi)^2 \int d^2q \; q^4 |u(\mathbf{q})|^2 \quad (4)$$

and

$$\int d^2x \; |u_{ij}| = 0. \quad (5)$$

For complete contact $u(\mathbf{x}) = h(\mathbf{x})$ and hence $u(\mathbf{q}) = h(\mathbf{q})$. Now, let us define the surface roughness power spectrum

$$C(q) = \frac{1}{(2\pi)^2} \int d^2x \; \langle h(\mathbf{x}) h(\mathbf{0}) \rangle {\rm e}^{-i\mathbf{q}\cdot\mathbf{x}}, \quad (6)$$

where $\langle ... \rangle$ stands for ensemble average. Note that

$$\langle |h(\mathbf{q})|^2 \rangle = \frac{A_0}{(2\pi)^2} C(q) \quad (7)$$

where A_0 is the (one side) surface area of the slab. Using (7) and that $u(\mathbf{q}) = h(\mathbf{q})$, and substituting (4) and (5) in (3) gives

$$U_{\rm el} = \frac{A_0 E}{24(1-\nu^2)} \int d^2q \; (qd)^3 q C(q) \quad (8)$$

Assume now instead that $\lambda << d$. In this case we can treat the elastic slab as infinitely thick when deriving the elastic energy stored in the slab, see Fig. 6 If we again assume that complete contact occurs between the solids, then $u_z = h(\mathbf{x})$, and as shown in Ref. [2,7],

$$U_{\rm el} = \frac{A_0 E}{4(1-\nu^2)} \int d^2q \; q C(q) \quad (9)$$

We can interpolate smoothly between the results (8) and (9) using the following expression for the elastic energy

$$U_{\rm el} = \frac{A_0 E}{4(1-\nu^2)} \int d^2q \; q C(q) \frac{(qd)^3}{6 + (qd)^3} \quad (10)$$

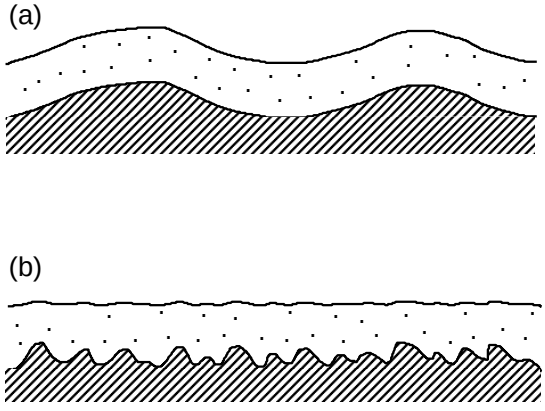

FIG. 6. (a) When the wavelength λ_0 of the surface roughness is much longer than the thickness d of the elastic slab, $\lambda_0 >> d$, the elastic slab deform so that the upper surface of the slab takes the same form as the substrate roughness profile. (b) When $\lambda_0 < d$ the upper surface of the slab is nearly flat (the displacement field decay as $u \sim \exp(-2\pi z/\lambda_0)$ with the distance z away from the substrate surface).

The adhesion energy is assumed proportional to the contact area so that assuming complete contact

$$U_{\rm ad} = -\Delta\gamma A_0 \tag{11}$$

The change in the free energy when the elastic slab moves in contact with the substrate is given by the sum of (10) and (11):

$$U_{\rm el} + U_{\rm ad} = -\gamma_{\rm eff} A_0 \tag{12}$$

where

$$\gamma_{\rm eff} = \Delta\gamma \left[1 - \frac{2\pi}{\delta}\int dq\ q^2 C(q) \frac{(qd)^3}{6+(qd)^3}\right] \tag{13}$$

where we have introduced the *adhesion length* $\delta = 4(1-\nu^2)\Delta\gamma/E$. The theory above is valid for surfaces with arbitrary random roughness, but will now be applied to (a) surfaces with roughness on a single length scale, (b) self-affine fractal surfaces, and (c) a sand paper surface for which the power spectra $C(q)$ has been calculated from the measured height profile $h(\mathbf{x})$.

(a). Assume surface roughness on a single length scale λ_0. This limiting case is not very realistic, but is very useful in order to understand some aspect of adhesion. We take

$$C(q) = C_0\delta(q - q_0) \tag{14}$$

where $q_0 = 2\pi/\lambda_0$. We can relate C_0 to the root mean square roughness amplitude using (6):

$$\langle h^2\rangle = \int d^2q\ C(q) = 2\pi C_0 q_0$$

Following earlier studies we define $h_0^2 = 2\langle h^2\rangle$ so that

$$C_0 = h_0^2/(4\pi q_0) \tag{15}$$

Substituting (14) in (13) and using (15) gives

$$\gamma_{\rm eff} = \Delta\gamma \left[1 - (q_0 h_0)^2 \frac{1}{2q_0\delta}\frac{(q_0 d)^3}{6+(q_0 d)^3}\right] \tag{16}$$

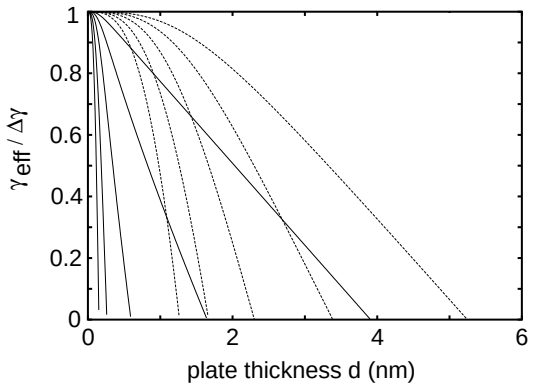

FIG. 7. The variation of the (normalized) effective interfacial free energy $\gamma_{\rm eff}$ with the thickness d of the plate. Results are shown for $q_1 = 10^9$ (dashed lines) and $q_1 = 10^{10}$ m^{-1} (solid lines) for $H = 0.5, 0.6, ..., 1$, where the magnitude of $\gamma_{\rm eff}$ monotonically increases with increasing H. In the calculation $\delta = 1$ Å.

(b). It has been found that many "natural" surfaces, e.g., surfaces of many materials generated by fracture, can be approximately described as self-affine surfaces over a rather wide roughness size region. A self-affine fractal surface has the property that if we make a scale change that is appropriately different along the two directions, parallel and perpendicular, then the surface does not change its morphology [8]. Recent studies have shown that even asphalt road tracks (of interest for rubber friction) are (approximately) self-affine fractal, with a long-distance cut-off length $\lambda_0 = 2\pi/q_0$ of order a few mm. For a self affine fractal surface [8] for $q > q_0$:

$$C(q) = \frac{H}{2\pi}\left(\frac{h_0}{q_0}\right)^2 \left(\frac{q}{q_0}\right)^{-2(H+1)}, \tag{17}$$

where $H = 3 - D_{\rm f}$ (where the fractal dimension $2 < D_{\rm f} < 3$), and where q_0 is the lower cut-off wavevector. For $q < q_0$ we take for simplicity $C(q) = 0$. The parameter h_0 determine the rms roughness amplitude, $\langle h^2\rangle = h_0^2/2$. We note that $C(q)$ can be measured directly, using many different methods, e.g., using stylus instruments or optical instruments.

Substituting (17) in (13) gives

$$\frac{\gamma_{\rm eff}}{\Delta\gamma} = 1 - (q_0 h_0)^2 \frac{1}{q_0\delta} f(H) \tag{18}$$

where

$$f(H) = H\int_1^{q_1/q_0} dx\ \frac{(q_0 d)^3 x^{3-2H}}{6+(q_0 d)^3 x^3} \tag{19}$$

The short distance cut wave vector cut off q_1 depends on the system under study. If it is assumed that the substrate is self affine fractal on all length scales, then $q_1 \approx 2\pi/a$, where a is of order a substrate lattice spacing, e.g., of order a few Angstrom. Thus the largest possible q_1 is $\approx 10^{10}$ m^{-1}. However, if the elastic solid has a thin very soft (say liquid-like) layer at its surface, as one of us has speculated before may be the case for the the lizard foot pad, then the effective cut off wave vector q_1 will be smaller. For example, if a $D \sim 60$ Å high mobility (liquid-like) layer occur then one expect $q_1 \approx 2\pi/D \approx 10^9$ m^{-1}. Similar if a thin (thickness D) (typically organic) contamination layer occur on the surface, which is able to rearrange itself at the interface and fill out nanoscale cavities, then again $q_1 \approx 2\pi/D$. In

some cases (e.g., for flies, beetles and other insects) a liquid substance is injecting in the contact area which will have a similar effect of acting as a large wave vector cut off in the q-integration in Eq. (19).

Let us apply Eq. (18) to the adhesion of a lizard toe to a rough substrate. The elastic modulus of keratin is in the range $1-4$ GPa and assuming the typical van der Waals surface energy difference [10] $\Delta\gamma \approx 1-3$ meV/Å^2 gives $\delta \approx 1$ Å. In Fig. 7 we show the calculated [from (18) and (19)] effective surface energy for a typical case. We have used $h_0 = 20$ nm, which was obtained from the measured height profile of a sand paper (the measurement refer to a linear dimension λ_0 of order a few hundred nanometers, i.e., to the lateral size of the leaf-like structure at the end of the spatula). We also used $q_0 = 2\pi/\lambda_0 \approx 10^7$ m^{-1} and $q_1 = 10^9$ (dashed lines) and 10^{10} m^{-1} (solid lines). Since the spatula-end consist of a plate-like structure with an average thickness of $d \approx 5-10$ nm it is clear that in the typical case of $H = 0.8$ the adhesion will be strongly suppressed (see also below). However, there is considerable uncertain in the value of δ (we have used $\delta = 1$ Å) since the elastic modulus E and the interfacial energy difference $\Delta\gamma$ have not been accurately measured until now. Similarly, the thickness of the leaf-plate will vary from a maximum at the basis, to a smaller value close to the periphery of the plate.

(c). Finally, let us present some numerical results for a sand paper surface for which we plan to study gecko-adhesion in the near future. We have measured the height distribution $h(\mathbf{x})$ using an Atomic Force Microscope. The measurement was performed over a rectangular area $L_x \times L_y$. Using a recently developed computer program [9] we have obtained the surface height distribution P_h and the surface roughness power spectra $C(q)$ from the height data.

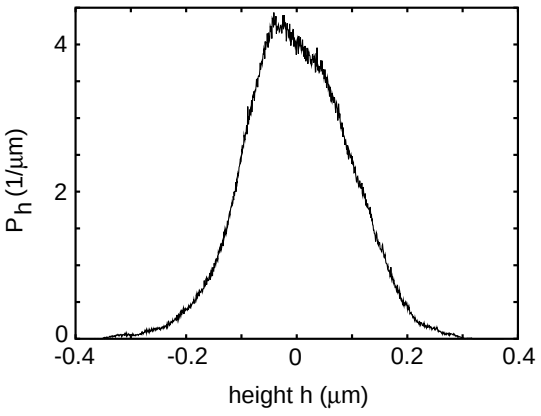

FIG. 8. The height probability distribution P_h for a sand paper (particle diameter ≈ 0.3 μm) surface with a root-mean-square roughness of about 93 nm.

In Fig. 8 we show the height probability distribution P_h for the sand paper surface with particle size of order 0.3 μm. The root-mean-square roughness 93 nm was measured over a surface area of the linear size $\lambda_0 \approx 30$ μm. Note that P_h is a near perfect Gaussian; one can show that randomly rough surfaces have Gaussian height distributions. Fig. 9 shows the surface roughness power spectra $C(q)$ for the same surface. The height profile was measured with a lateral resolution $a = 29.3$ nm, corresponding to the wave vector $q \approx \pi/a \approx 10^8$ m^{-1}; in Fig. 9 we have made a linear extrapolation to larger q vectors. Note that $C(q)$ has a power law region (i.e., a linear region between log$C$ and log$q$), characterized by the exponent $H \approx 1.1$.

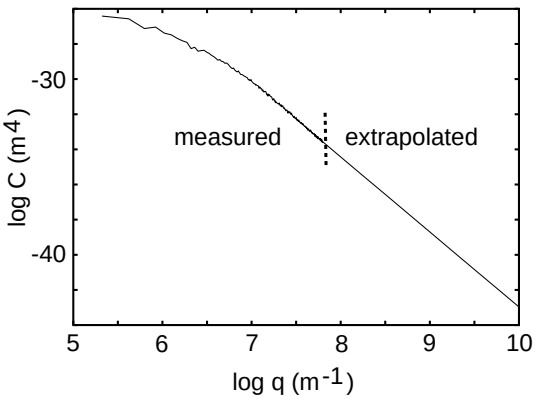

FIG. 9. Surface roughness power spectra $C(q)$ as a function of the wave vector q for the same sand paper surface as in Fig. 8.

Fig. 10 shows the variation of the (normalized) effective interfacial free energy $\gamma_{\rm eff}$ with the thickness d of the plate. Curves a-d correspond to different short distance cut off wavevector q_1, namely a: 10^7, b: 10^8, c: 10^9 and d: 10^{10} m^{-1}. In the calculation we have used the power spectra $C(q)$ shown in Fig. 9, and $\delta = 1$ Å. It is interesting to note that using the large wave vector cut off $q_1 = 10^9$ or 10^{10} m^{-1} gives nearly the same result. This implies, e.g., that at least in the present case a very soft thin (nanometers) layer at the interface will not increase the adhesion to any appreciate extent, i.e., such a layer may not be necessary in order for the lizard to adhere to rough substrates.

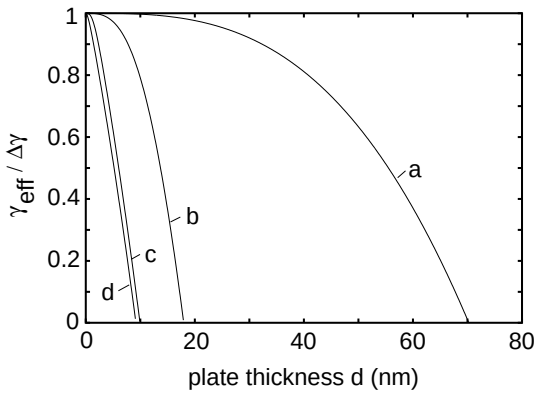

FIG. 10. The variation of the (normalized) effective interfacial free energy $\gamma_{\rm eff}$ with the thickness d of the plate. Curves a-d correspond to different short distance cut off wavevector q_1, namely a: 10^7, b: 10^8, c: 10^9 and d: 10^{10} m^{-1}. For the power spectra $C(q)$ shown in Fig. 9 and with $\delta = 1$ Å.

The curves in Fig. 10 was calculated using Eq. (13) with the power spectra $C(q)$ shown in Fig. 9, which start at $q_0 \approx 2.1 \times 10^5$ m^{-1}. However, when studying the adhesion between the lizard leaf-like plate and the substrate we should only include roughness components with wavelength shorter than the lateral size of the leaf-plate, which is of order $\lambda_0 \approx 300$ nm. In Fig. 11 we compare the results from Fig. 10 (curves b-d) with the effective surface energy obtained when we only include roughness wavevector components with $q > q_0 = 2\pi/\lambda_0 \approx 2 \times 10^7$ m^{-1} (dashed lines). The thickness of the plate-like structure at the end of the spatula is in the range of $d \approx 5 - 10$ nm so based on Fig. 11 (curve d) one would expect to observe a strong decrease in the adhesion on this surface as compared to a perfectly smooth substrate (see also Sec. 4). Experiments to check the predictions above is currently underway. An accurate comparison between theory and experiment would, however, require that the height profile $h(\mathbf{x})$ is measured with higher resolution (~ 3 nm) so that $C(\mathbf{q})$ can be calculated at least up to $q \sim 10^9$ m^{-1}, rather than extrapolated to large q as in the present case (see Fig. 9).

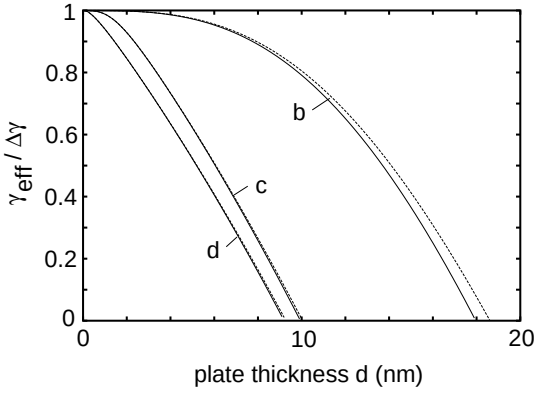

FIG. 11. The variation of the (normalized) effective interfacial free energy $\gamma_{\rm eff}$ with the thickness d of the plate. Curves b-d correspond to different short distance cut off wavevector q_1, namely b: 10^8, c: 10^9 and d: 10^{10} m^{-1}. For the power spectra $C(q)$ shown in Fig. 9 and with $\delta = 1$ Å. The solid curves are the same as in Fig. 10 while the dashed curves are obtained by only including roughness wavelength components $q > q_0 = 2 \times 10^7$ m^{-1}.

4. Comments

In this section we make two comments related to the theory presented above. First, note that when detached regions are included, the effective interfacial energy as function of the thickness d of the slab will have a tail toward larger d. This is shown schematically in Fig. 12(dashed line) for case b in Fig. 10. We plan to study this effect in detail in the future by generalizing the theory presented in Ref. [2], which is valid for semi-infinite solids rather than plates.

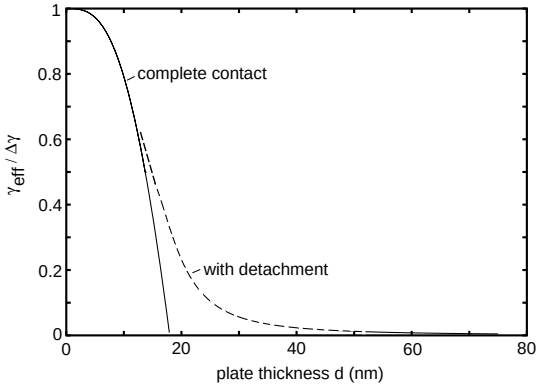

FIG. 12. When detached regions are included, the effective interfacial energy as function of the thickness d of the slab will have a tail toward larger d. For the case b in Fig. 10 (schematic).

However, even when the minimum free energy state correspond to complete contact, the elastic plate may (because of friction) be trapped in a metastable state as illustrated in Fig. 13. In this case, because the kinetic friction is smaller than the static friction, sliding or vibrating the plate may increase the contact area. This effect is known experimentally: by sliding the lizard toe pad for a short distance the adhesion force can be increased [3].

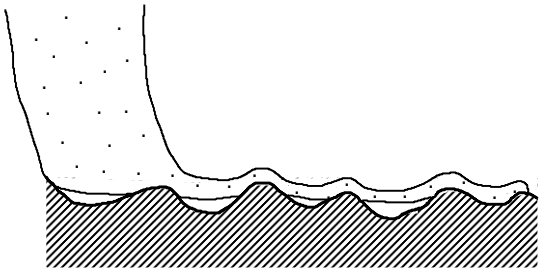

FIG. 13. The free energy is minimal for the complete contact state but because of friction the plate is not able to deform to follow the substrate.

Measurements have shown that the friction between a beetle (Gastrophysa viridula) adhesive pad, and the sand paper surface discussed in Sec. 3(c), is about 5 times smaller than on the smooth substrate (of the same material). One interpretation of this result is that the area of real contact may be ~ 5 times smaller on the rough substrate compared to the smooth substrate. The theory presented in this paper *assume* complete contact, but when the theory predict $\gamma_{\rm eff}/\Delta\gamma << 1$ (as in Sec. 3) one may, in fact, expect only partial contact (see above); this would be consistent with the beetle friction data. When sand paper with larger particles was used (> 1 μm) the friction was nearly the same as on the smooth substrate, indicating complete contact in these cases. Unfortunately, no AFM data of the height profile was reported for these cases.

It has been pointed out that on a smooth surface only 0.03% of the gecko's setae are necessary in order to support its body weight, and the question has been raised why the geckos are so over-built [3]. However, it is clear from the calculations presented in Sec. 3 and from Fig. 12 that on a rough substrate the spatulae-substrate adhesion may be strongly reduced, and we believe that this may be the main reason for why the gecko's adhesive system is so apparent over-built.

5. Discussion

How can a fly or a cricket walk on a glass window, or a lizard move on a stone or concrete wall? In order to explain the observed adhesion, these questions can be reformulated as follows: how is the extremely soft surface layer, which must exist on the adhesion pads, designed. This fundamental question has interested scientists for many years, and recently very important work has been performed in order to gain a deeper insight into this problem [1]. Thus it is now known that the adhesive systems, adapted to attachment to a variety of surfaces, are build in a hierarchic manner from fibers and plates with very small bending elasticities, making it possible for the molecular attraction at the interface to pull the two surfaces into nearly complete contact without storing up a large elastic deformation energy at the interface.

In this paper we have focus on dry adhesion which seams to be relevant for lizards [3]. In Ref. [5] one of us has presented a simple model study of fiber adhesion on surfaces with roughness on many length scales, and applied it to the adhesion between a lizard toe and a smooth or rough hard substrate. In this paper we have extended that study, and considered the spatula-plate adhesion.

Naturally occurring surfaces (e.g., a stone wall) have surface roughness on all length scales, from macroscopic to atomic. Adhesion between two bodies is only possible if the surfaces are able to deform (elastically or plastically) to make direct (atomic) contact at a non-negligible fraction of the nominal contact area. For "hard" solids this is nearly impossible and as a result adhesion is usually negligible between hard rough surfaces [11].

The skin of the gecko toe-pad is able to deform and follow the substrate roughness profile on length scales much longer than the thickness $d \approx 100$ μm of the elastic keratin film, say beyond ~ 1000 μm. At shorter length scales the keratin film, because of its high elastic modulus (of order 1 GPa), can be considered as rigid and flat. Elastic deformation of the pad surface on length scales shorter than ~ 1000 μm, involves the compliant setae fiber array system, with fibers of thickness ~ 4 μm. In Ref. [5] we have shown that if the surface roughness root-mean-square amplitude, measured over a patch $D \times D$ with $D \approx 1000$ μm, is smaller than a characteristic length (the adhesion length) (see Ref. [5]), then the fiber array system is able to deform (without storing in it a lot of elastic energy) to follow the surface roughness in the wavelength range $10 < \lambda < 1000$ μm. However, if the setae fiber tips would be blunt and compact they would not be able to penetrate into surface "cavities" with diameter less than a few μm. Thus, negligible atomic contact would occur between the surfaces, and the adhesion would be negligible. For this reason, at the tip of each long (thick) fiber occur an array of ~ 1000 thinner fibers (diameter of order ~ 0.1 μm). These fibers are able to penetrate into surface roughness cavities down to a length scales of a few tenth of a micrometer. However, if the thin fibers would have blunt and compact tips made from the same "hard" keratin as the rest of the fiber, then one would still obtain a very small adhesion, since a lot of elastic energy would be necessary to deform the surfaces of the thin fibers to make atomic contact with the substrate. Therefore the top of the thin fibers end with thin leaf-like plates, which can be easily bent (without storing a lot of elastic energy) to follow the surface roughness profile. In Ref. [5] one of us speculated that the spatula tips are covered with a very soft compliant layer, e.g., a liquid-like (high mobility) layer of polymer chains grafted to the tip of the thin fibers. This liquid-like layer, if thick enough, would be able to adjust to the substrate roughness profile over lateral distances below ~ 10 nm. However, the calculation presented above (Fig. 10 and 11), indicate that such a layer may not always be necessary in order for strong

adhesion to occur. However, the calculations presented in Fig. 6 shows that for rough surfaces with the fractal dimension $D_{\rm f} = 3 - H > 2.2$ very small adhesion may occur in most cases.

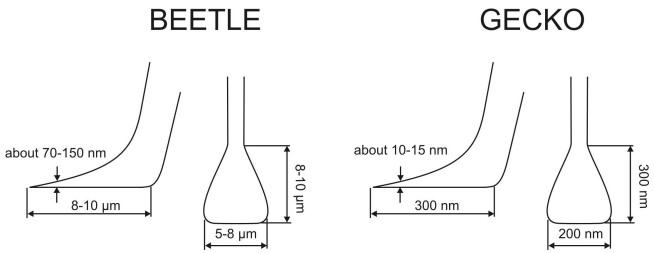

FIG. 14. The adhesive system beetle and lizards.

Finally, let us notice that lizards are the most heavy living objects on this planet that are able to adhere to, e.g., a rough vertical stone wall. Since the surface area of a body increases slower than the volume (or mass) with the increase of the linear size of the body, it is clear that the adhesive system in large living bodies such as lizards, must be more effective (per unit attachment area) than in smaller living objects such as flies or beetles [1]. This most likely implies that lizards have the most effective adhesive systems appeared in the biological evolution for the purpose of locomotion. This is confirmed by electron microscopy studies. Let us compare the spatulae of the adhesive systems of beetles with lizards (Fig. 14). Note that the spatulae are thinner in lizards than in beetles. Also the diameter of terminal branches is smaller. This implies that less elastic energy per unit surface area will be stored in the lizard adhesive system, and that the effective interfacial energy $\gamma_{\rm eff}$ will be larger for lizards than for beetles.

6. Summary and conclusion

We have studied the adhesion of elastic plates to rough substrates, which is relevant to biological systems, e.g., flies, crickets and lizards, where the adhesive microstructures consist of a hierarchical arrays of thin fibers and plates. The effective elastic modulus of the fiber–plate arrays is very small on all relevant length scales (from mm to nm), which is of fundamental importance for adhesion on rough substrates. We have shown how the adhesion depend on the nature of the substrate roughness, and applied the theoretical results to the adhesion pads of lizards. Experiments to test the theoretical results are underway. Finally, we note that the construction of man-made adhesives based on fiber and plate arrays may be an attractive alternative to the usual adhesives based on thin polymer films. Some pioneering experiments have indeed shown enhanced adhesion for fiber array systems, but no man-made system of the hierarchic nature used in biological systems have so far been produced [12,13].

Acknowledgments B.P. thanks the EC for a "Smart QuasiCrystals" grant under the EC Program "Promoting Competitive and Sustainable GROWTH". S.G. wish to thank A. Peressadko for AFM data. This work was supported by the Federal Ministry of Education, Science and Technology, Germany (project BioFuture 0311851).

[1] M. Scherge and S. Gorb, *Biological Micro- and Nanotribology*, Springer, Berlin (2001).
[2] B.N.J. Persson, Eur. Phys. J. E**8**, 385 (2002); Phys. Rev. Lett. **89** 245502 (2002)
[3] K. Autumn, M. Sitti, Y.A. Liang, A.M. Peattie, W.R. Hansen, S. Sponberg, T.W. Kenny, R. Fearing, J.N. Israelachvili and R.J. Full, Evolution, PNAS Early Edition; K. Autumn, Y.A. Liang, S.T. Hsieh, W. Zesch, W.P. Chan, T.W. Kenny, R. Fearing and R.J. Full, Nature **405**, 681 (2000).; K. Autumn and A. Peattie, *Mechanisms of Adhesion in Geckos*, Int. Comp. Bio. **42** (2002); S. Sponberg, W. Hansen, A. Peattie and K. Autumn, *Dynamics of isolated gecko setal arrays*, Int. Comp. Bio. 39:395 (2002).
[4] K.N.G. Fuller and D. Tabor, Proc. R. Soc. London, Serie A**345**, 327 (1975).
[5] B.N.J. Persson, J. Chem. Phys. **118**, 7614 (2003)
[6] L.D. Landau and E.M. Lifshitz, *Theory of Elasticity* (Pergamon Press, London, 1959).
[7] B.N.J. Persson and E. Tosatti, J. Chem. Phys. **115** 5597 (2001).
[8] J. Feder, *Fractals* (Plenum Press, New York, 1988).
[9] B.N.J. Persson, unpublished
[10] J.N. Israelachvili, *Intermolecular and Surface Forces* (Academic Press, London, 1995).
[11] B.N.J. Persson, *Sliding Friction: Physical Principles and Applications*, second edition (Springer, Heidelberg, 2000).
[12] A. Peressadko and S.N. Gorb, subm. to J. Adhesion.
[13] A.K. Geim, S.V. Dubonos, I.V. Grigorieva, K.S. Novoselov, A.A. Zhukov and S.Yu. Shapoval, Nature (2003)